

Extended Abstract

# Investigation of the Film Thickness Influence on the Sensor Response of In<sub>2</sub>O<sub>3</sub>-Based Sensors for O<sub>3</sub> Detection at Low Temperature and Operando DRIFT Study <sup>†</sup>

Daniele Ziegler <sup>1,\*</sup>, Paola Palmero <sup>1</sup>, Jean-Marc Tulliani <sup>1</sup>, Anna Staerz <sup>2</sup>, Alexandru Oprea <sup>2</sup>, Udo Weimar <sup>2</sup> and Nicolae Barsan <sup>2</sup>

<sup>1</sup> Politecnico di Torino, Department of Applied Science and Technology, INSTM R.U PoliTO-LINCE Laboratory, Corso Duca degli Abruzzi, 24, 10129 Torino, Italy; paola.palmero@polito.it (P.P.); jeanmarc.tulliani@polito.it (J.-M.T.)

<sup>2</sup> Institute of Physical and Theoretical Chemistry (IPTC), University of Tuebingen, Auf der Morgenstelle 15, D-72076 Tuebingen, Germany; anna.staerz@ipc.uni-tuebingen.de (A.S.); alexandru.oprea@ipc.uni-tuebingen.de (A.O.); upw@ipc.uni-tuebingen.de (U.W.); nb@ipc.uni-tuebingen.de (N.B.)

\* Correspondence: daniele.ziegler@polito.it

<sup>†</sup> Presented at the 8th GOSPEL Workshop. Gas Sensors Based on Semiconducting Metal Oxides: Basic Understanding & Application Fields, Ferrara, Italy, 20–21 June 2019.

Published: 19 June 2019

---

Industrial pollution and traffic emissions emit dangerous amounts of O<sub>3</sub>, NO<sub>2</sub>, VOCs and PM into environment, bringing higher incidence of morbidity and mortality in respiratory sicknesses [1]. Among tropospheric pollutant species, monitoring the O<sub>3</sub> concentration is remarkably important for its toxicity. The aftereffects of O<sub>3</sub> exposure indeed are upper respiratory irritation, rhinitis, cough, headache, occasional nausea, and vomiting [2]. In 2015, the United States Environmental Protection Agency (EPA), reinforced the National Ambient Air Quality Standards (NAAQS) for O<sub>3</sub> at ground-level not to exceed 70 ppb to improve the protection of human health [3].

This work presents n-type In<sub>2</sub>O<sub>3</sub> as sensitive material to detect O<sub>3</sub> between 0.1 and 1 ppm at low temperatures (75 °C–150 °C). In<sub>2</sub>O<sub>3</sub> powders were synthesized by hydrothermal route [4], with the goal to achieve a finer crystallite size, higher specific surface area and lower degree of agglomeration compared to commercial In<sub>2</sub>O<sub>3</sub> (Sigma Aldrich, St. Louis, MO, USA). Those characteristics are essential to enhance the sensor performances [5].

In the synthesis, In<sub>2</sub>O<sub>3</sub> nanostructures were realized by hydrothermal method using indium nitrate as indium precursor, soda as mineralizer and CTAB as capping agent, according to previous literature [6]. The mixture was maintained for 24 h at 70 °C and then for 12 h at 120 °C. Subsequently, powders were calcined at 400 °C for 30 min obtaining In<sub>2</sub>O<sub>3</sub> [4].

In<sub>2</sub>O<sub>3</sub> powders were characterized by laser granulometry, Thermal Analysis, X-ray Diffraction, N<sub>2</sub> adsorption, Field Emission-Scanning Electron Microscopy and High-Resolution Transmission Electron Microscopy.

Sensors were fabricated by screen-printing technique onto  $\alpha$ -alumina substrates with Pt electrodes and a backside Pt heater. Inks for screen-printing were realized by mixing In<sub>2</sub>O<sub>3</sub> powders with ethylene glycol monobutyl ether (Emflow), as organic vehicle and polyvinyl butyral (PVB) acting as temporary binder. After screen-printing deposition sensors were dried at 80 °C overnight and fired at 500 °C for 1 h in air. For obtaining different layer thicknesses in the range 10–100  $\mu$ m, the first layer was dried and then a new layer was printed onto it.

Films were characterized by Scanning Electron Microscopy, electrical measurements and *operando* diffuse reflectance infrared Fourier transform (DRIFT) spectroscopy.

Sensors were tested towards different amounts of O<sub>3</sub>, NO<sub>2</sub> and H<sub>2</sub> under 0, 30% and 60% of RH (relative humidity) to study the selectivity of the as-realized chemical sensors for O<sub>3</sub> detection. Best results were achieved at 150 °C towards O<sub>3</sub>, with the sensor selectivity for O<sub>3</sub> increasing by increasing the working temperature from 75 °C to 150 °C. Both oxidant gases (O<sub>3</sub> and NO<sub>2</sub>) showed best performance at higher RH amounts, whereas for H<sub>2</sub> the trend was opposite, probably due to the competition between H<sub>2</sub> and H<sub>2</sub>O for the same adsorption sites on the In<sub>2</sub>O<sub>3</sub> surface. At 150 °C, under 1 ppm O<sub>3</sub>, the variation of film resistance is 5 orders of magnitude, while it was only equal to 2 orders of magnitude under 1 ppm of NO<sub>2</sub>. Under 30% RH, the influence of sensor thickness is much higher under O<sub>3</sub> compared to NO<sub>2</sub> and a logical trend was noticed in which by changing one order of magnitude the sensor thickness, the sensor response varies of more than 3 orders of magnitude under 1 ppm O<sub>3</sub>. Under NO<sub>2</sub>, only a small influence of the sensing film thickness on the sensor response was detected. Finally, the interference with H<sub>2</sub> is negligible as the sensor response towards H<sub>2</sub> is independent from the film thickness, as expected. Calibration curves of In<sub>2</sub>O<sub>3</sub> sensor towards O<sub>3</sub>, NO<sub>2</sub> and H<sub>2</sub> at 150 °C and 30% RH in the range 10–100 μm of thickness are displayed in Figure 1.

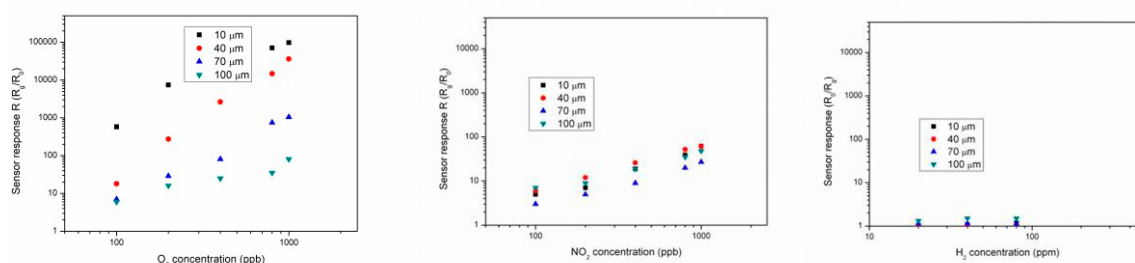


**Figure 1.** Comparison between 10, 40, 70 and 100 μm thick In<sub>2</sub>O<sub>3</sub> sensor response towards O<sub>3</sub> (left), NO<sub>2</sub> (center) and H<sub>2</sub> (right) at 150 °C and 30% RH.

By DRIFTS, the aim is to clarify the interaction of NO<sub>2</sub> and O<sub>3</sub> with In<sub>2</sub>O<sub>3</sub> surface establishing tightly the relationship between surface structure and adsorbed species with the gas sensing response.

Considering the NO<sub>2</sub>-In<sub>2</sub>O<sub>3</sub> interaction, the OH groups, most likely due to adsorbed water on the In<sub>2</sub>O<sub>3</sub> surface, play a key role in the NO<sub>2</sub> adsorption. NO<sub>2</sub> withdraw more electrons from In<sub>2</sub>O<sub>3</sub> in the presence of water forming nitrites and resulting in the measured increased in electrical resistance. This is confirmed by the higher increase in electrical resistance under humid atmospheres. OH groups are consumed when NO<sub>2</sub> is adsorbed onto the surface in the form of nitrites and in this process, H bonds are broken.

In the interaction of O<sub>3</sub> with In<sub>2</sub>O<sub>3</sub> surface, signals related to peroxide formation during O<sub>3</sub> adsorption and decomposition were detected as well as peaks due to physisorbed O<sub>3</sub> still present at 150 °C. Furthermore, bands generated by carbonate-like species formed through reactions of O<sub>3</sub> with residual carbonaceous impurities from the synthesis route were recognized.

To conclude, in this work the role of the film thickness under O<sub>3</sub>, NO<sub>2</sub> and H<sub>2</sub> exposure was studied for In<sub>2</sub>O<sub>3</sub> sensor realized by screen printing technique. Finally, by *operando* DRIFT a complex sensing mechanism has been evidenced for In<sub>2</sub>O<sub>3</sub> sensors, involving OH groups and adsorbed water in the mechanism of NO<sub>2</sub> adsorption and peroxide formation and O<sub>3</sub> physisorption during O<sub>3</sub> exposure.

## References

1. Brunekreef, B.; Holgate, S.T. Air pollution and health. *Lancet* **2002**, *360*, 1233–1242, doi:10.106/S0140-6736(02)11274-8.
2. Gottschalk, C.; Libra, J.A.; Saupe, A. *Ozonation of Water and Waste Water—A Practical Guide to Understanding Ozone and Its Applications*; Wiley: Weinheim, Germany, 2000.

3. 2015 National Ambient Air Quality Standards (NAAQS) for Ozone. Available online: <https://www.epa.gov/ozone-pollution/2015-national-ambient-air-quality-standards-naaqs-ozone> (accessed on 7 April 2019).
4. Shinde, D.V.; Ahn, D.Y.; Jadhav, V.V.; Lee, D.Y.; Shrestha, N.K.; Lee, J.K.; Lee, H.Y.; Maneb, R.S.; Han, S.H. A coordination chemistry approach for shape controlled synthesis of indium oxide nanostructures and their photoelectrochemical properties. *J. Mater. Chem. A* **2014**, *2*, 5490–5498.
5. Korotcenkov, G.; Brinzari, V.; Cerneavski, A.; Ivanov, M.; Golovanov, V.; Cornet, A.; Morante, J.; Cabot, A.; Arbiol, J. The influence of film structure on In<sub>2</sub>O<sub>3</sub> gas response. *Thin Solid Films* **2004**, *460*, 315–323.
6. Yan, T.; Wang, X.; Long, J.; Liu, P.; Fu, X.; Zhang, G.; Fu, X. Urea-based hydrothermal growth, optical and photocatalytic properties of single-crystalline In(OH)<sub>3</sub> nanocubes. *J. Colloid Interface Sci.* **2008**, *325*, 425–431.



© 2019 by the authors. Licensee MDPI, Basel, Switzerland. This article is an open access article distributed under the terms and conditions of the Creative Commons Attribution (CC BY) license (<http://creativecommons.org/licenses/by/4.0/>).